

Analysis of Cardiac Mri To Find Out Cardiovascular Disease Using Automatic Segmentation Techniques

Mr. Kayte Jaypalsing Natthusing¹, Mr. Sangramsing N.Kayte²,
Sumegh S. Tharewal³, Mohammed Waseem Ashfaque⁴,

^{1, 2, 3}(Department of Computer Science & IT, Dr. Babasaheb Ambedkar Marathwada University, Aurangabad
(MH), India.)

⁴(Department of IT, Buraimi University College, Buraimi, Oman)

Abstract : We are study and experimental work is show this paper how automatically work SIOX techniques for got the good result. For the last 20 years, Magnetic Resonance Imaging (MRI) has become a reference examination for cardiac morphology, function and perfusion in humans. Yet, due to the characteristics of cardiac MRI and to the great variability of the images among patients, the problem of heart cavities segmentation in MRI is still open. This paper is a focuse of fully and semi-automated methods performing segmentation in short axis images using a cardiac cine MRI sequence. Medical background and specific segmentation difficulties associated to these images are presented. For this particularly complex segmentation task, prior knowledge is required. We thus propose an original categorization for cardiac segmentation methods, with a special emphasis on what level of external information is required (weak or strong) and how it is used to constrain segmentation. After reviewing method principles and analyzing segmentation results, we conclude with a discussion and future trends in this field regarding methodological and medical issues using simple iterative Object extraction (SIOX), we are got the result is endocardium / epicardium $4.84E.03 / 9.67E+03(M) 2.33E03 / 3.94E.03 (SD)$, this techniques are give the best result for segmentation of Left ventricle cardiac MRI .

Keyword: Cardiac MRI, Left- Ventricle Segmentation, M=Mean, SD= Standard Deviation

I. Introduction

1.1. PROBLEM DESCRIPTION

Cardiovascular diseases are the leading cause of death worldwide [4]. The quality of patient diagnosis and prognosis depends on the accurate measurement of cardiac properties, which can be derived from annotations of images of the cardiac structure. Annotation by human specialists in modalities such as magnetic resonance imaging is a time intensive process. Additionally, when papillary muscles are close to the endocardium a strong edge is absent which can lead to inconsistent annotations. Accurate segmentation therefore needs integration of spatial and temporal information. Since only one frame is annotated at a time, it is difficult for a human to take temporal information into account during annotation.

Automation of the segmentation process therefore has numerous benefits, even if used only to support and not fully replace a human annotator. A number of automated segmentation techniques exist, but the integration of spatial and temporal information remains challenging. These challenges are addressed in this study.

II. Background

2.1. Cardiac MRIs

The heart's primary function is that of receiving oxygen poor blood from the body, moving it through the lungs and then distributing the oxygenated blood to the rest of the body. Figure 1.1 illustrates a short-axis view of the basic cardiac structure.

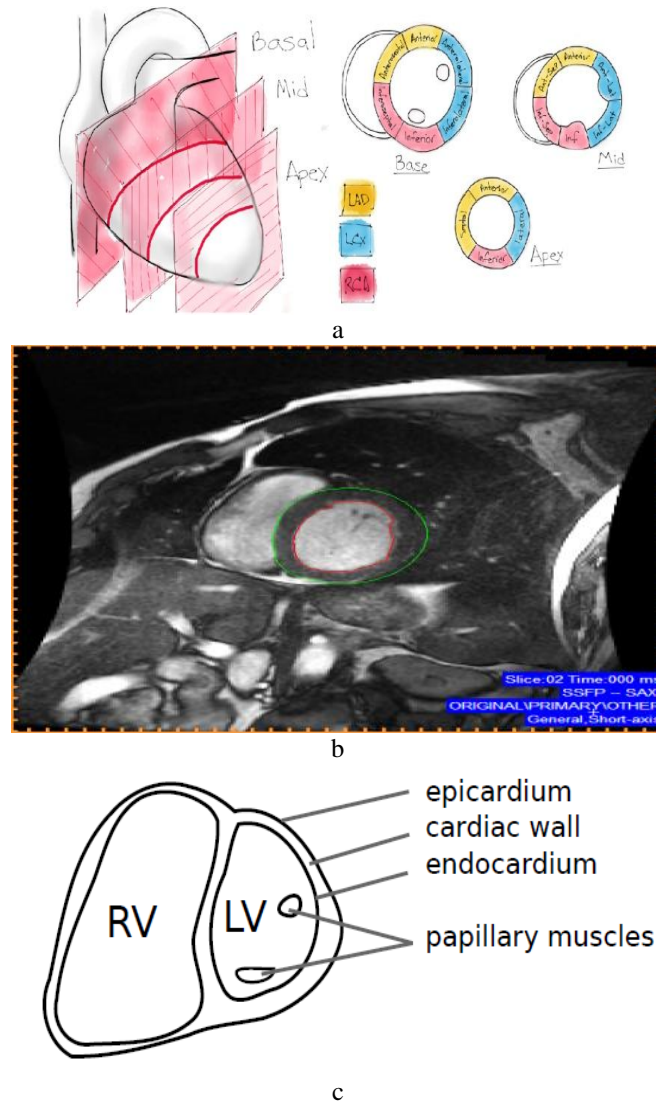


Figure 1.1: Simplified diagram of the left and right ventricles Structure (a) Basal, Mid, Apex Cardiac view (b) Original cine (b) RV and LV Mask information Structure.

Stated simply, the right ventricle receives de-oxygenated blood from the body during ventricle relaxation (diastole) and pumps it to the lungs on contraction (systole). Simultaneously oxygenated blood is received from the lungs into the left ventricle during diastole and forced to the rest of the body on systole. The left ventricle therefore operates at a higher pressure than the right and consequently has more muscle mass.

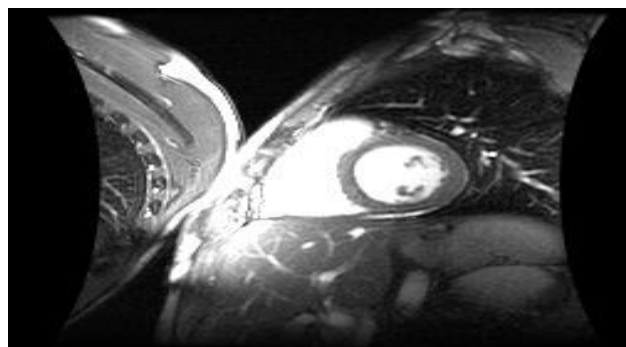


Figure 1.2: MRI short axis view of cardiac ventricles and surrounding structure.

Figure 1.2 shows a Magnetic Resonance Imaging (MRI) short-axis view of the cardiac ventricles and their surrounding structure. Magnetic Resonance Imaging is used in the visualization of internal structure by producing images where high pixel intensity corresponds to higher water content.

Cardiac MRI has a number of important advantages when compared to alternative imaging modalities such as X-ray computed tomography and ultrasound. It is non-invasive, does not emit ionizing radiation, can be used with multiple imaging planes and has a wide topological field of view. Additionally, as MRIs respond to water content it can be used to produce images that have a high discriminative contrast between blood, the myocardium and surrounding soft tissues. Magnetic Resonance Imaging can also produce a series of images in succession.

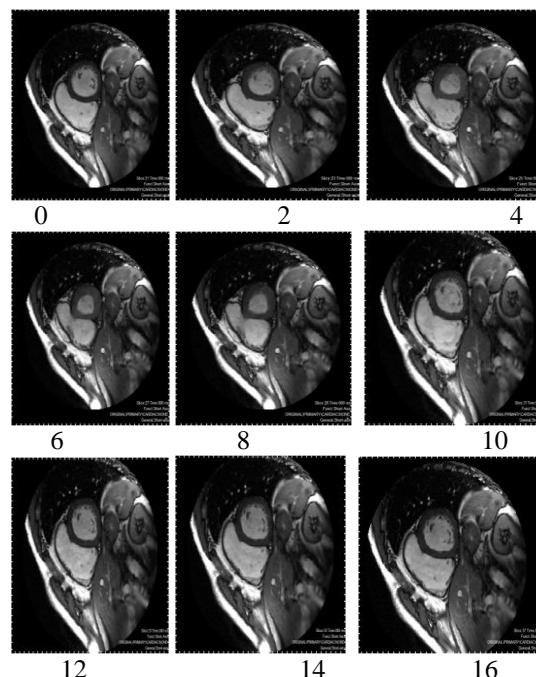


Figure 1.3 contains frames from a video sequence of MRI short axis view of the cardiac ventricles, synchronized to a single cardiac cycle. The left ventricle undergoes contraction (systole) in the images $T = 0 \dots 8$ and relaxation (diastole) during $T = 9 \dots 16$.

The direction of blood flow through the ventricles is controlled by heart valves. The opening and closing of the valves are driven by the pressure gradient across the valves. Papillary muscles (Figures 1.1 and 1.2) and chordae tendineae (“heart strings”), inside the ventricles, prevent the valves from inverting, which could cause backward flow of blood from the ventricles into the atria.

2.2. MRI capture and annotation

The cardiac MRI acquisition protocol often requires that the subject holds their breath while a video sequence of successive images is taken. Focus of the MRI instrumentation is then moved to a different short axis slice and the acquisition is repeated. If the subject breathes between different slices, then, due to different levels of inhalation and expiration, the cardiac structure can undergo significant displacement. For this reason we have not integrated information from different spatial slices into our model and focus only on the annotation of temporal sequences of images for a single slice, as shown in Figure 1.3. The properties of the left ventricle, such as volume, ejection fraction [5] and wall thickness are important indicators for the diagnosis and prognosis of many heart-related problems. Motion and deformation descriptors also include ventricle boundary wall motion, endocardium motion, wall thickening and strain analysis. Many of these are conveniently extracted from Magnetic Resonant Images (MRIs). The calculation of these properties requires accurate annotation of the left ventricle to isolate it from its surrounding structure. Figure 1.4 contains an example of human annotated inner and outer contours of the left ventricle in a single image.

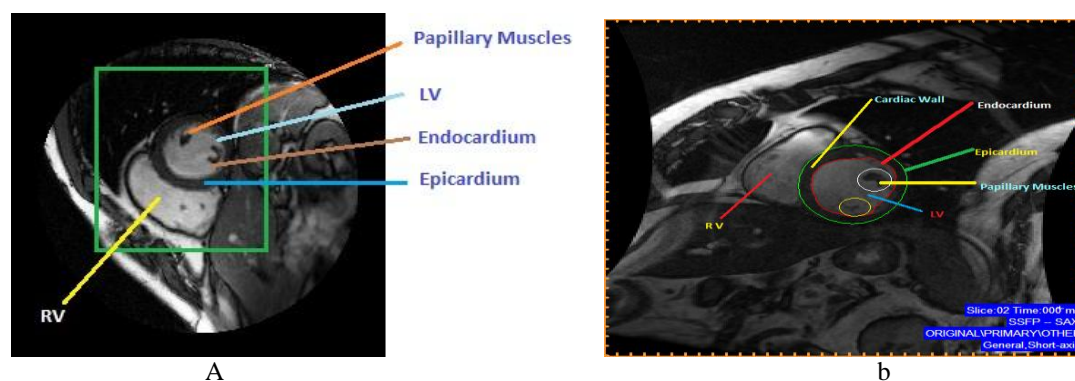


Figure 1.4: MRI short axis view of ventricles with human annotated (inner and outer) contours shown in red and green. Surrounding tissue is omitted for illustrative purposes.

Manual annotation is a tedious process and lacks consistency between human annotators [1, 3] and even between separate annotations by the same annotator. This problem primarily arises from the apparent ambiguity as to the extent to which the papillary muscles influence and, possibly, obscure the endocardium border. For research on the effects that discrepancies in annotations of the papillary muscles can have on the calculation of left ventricle function and mass see e.g. [2, 3, 6]. When modeling the structural properties of the ventricle wall, it is often desirable to include these muscles inside the inner contour. The examples in Figure 1.5 illustrate the presence of papillary muscles close to the endocardium border and a human annotator's segmentation. From inspection of the human annotation, it is clear that the presence of the endocardium border is inferred from prior external information of the motion and shape of the ventricle, and not only from what is available in the image itself, such as strong intensity gradients. Such considerations are likely to lead to inconsistencies, in particular when there is little difference between the intensity of the endocardium and surrounding structure.

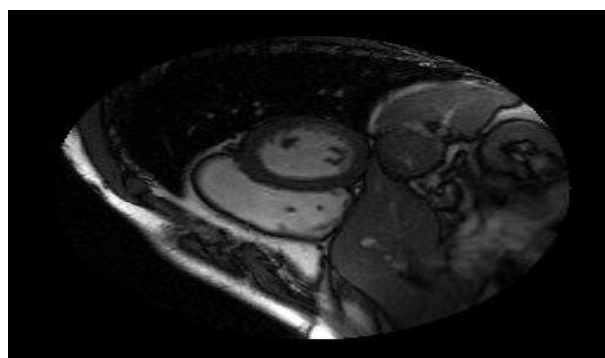


Figure 1.5: Presence of papillary muscles obscure the edge of the inner contour due to its similar intensity to the cardiac wall. Human annotated inner and outer contours are shown in yellow. Surrounding tissue is cropped for clarity.

2.3. MRI and Cardiac Anatomy

Magnetic Resonance Imaging (MRI) offers a non-invasive way to quickly acquire accurate images of the interior of the human body. Figure 1.6 depicts an MRI scanner. When compared with other imaging modalities such as X-rays, the main advantage of MRI is that the radiation it uses to acquire images is mostly non-ionizing [7]. Non-ionizing radiation does not have enough energy to remove tightly bound electrons. According to current scientific knowledge, most of the potentially harmful radiation falls in the range of ionizing radiation, and MRI does not carry some of the health related hazards associated with other imaging modalities such as X-rays.

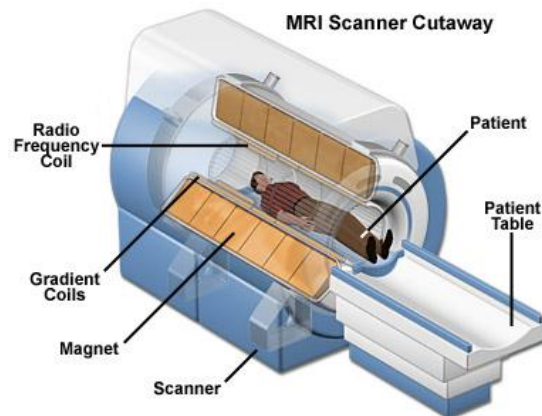


Figure 1.6: Example of an MRI Scanner. Copied from <http://www.magnet.fsu.edu/education/tutorials/magnetacademy/mir/>

Other common imaging techniques such as Ultrasound, do not offer as high quality images as MRI does, and do not have the soft tissue discrimination abilities of MRI. For this reason MRI is currently the best method for cardiac diagnosis.

The heart is a muscle that contracts and expands under the influence of electrical pulses. The average adult heart (figure 1.7) is roughly the size of a fist. It consists of four chambers, namely, the left atrium, the right atrium, the left ventricle (LV), and the right ventricle (RV).

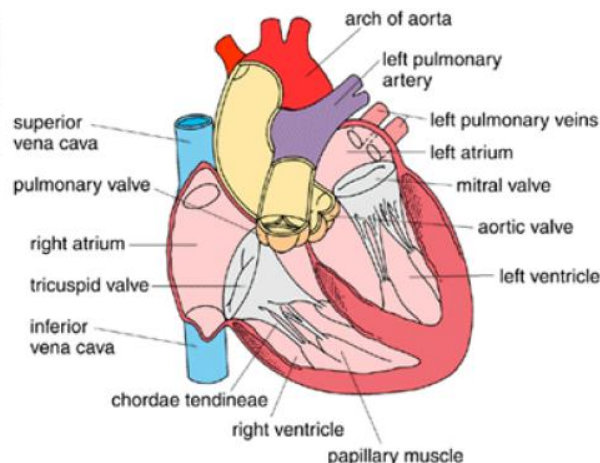


Figure 1.7: Long Axis view of the heart. The myocardium consists of the dark pink colored region. Figure copied from <http://www.marthajefferson.org/modules/cardiac/anatomy.htm>

At these chambers there are four one-way valves that ensure the blood flows in the right direction. These are the mitral valve, tricuspid valve, aortic valve and pulmonary valve as shown in figure 1.7. The two atria receive blood from outside the heart and then pump it to the ventricles, and the two ventricles in turn, pump the received blood outside of the heart. The right ventricle receives de-oxygenated blood and pumps it to the lungs to oxygenate it, and the left ventricle receives oxygenated blood and pumps it through the body. Problems with cardiac performance tend to present themselves in the left ventricle (LV) much more often than they do in the right ventricle (RV). For this reason most research on cardiac image analysis has focused on the left ventricle of the heart, an approach we will also be following in this paper.

The heart is composed of 3 main tissue layers and the endocardium, the myocardium, and the epicardium.

- A. The endocardium is a thin lining of the interior walls of the LV and RV.
- B. The myocardium is a thick layer (shown in dark pink color in figure 1.7) of muscle cells that can contract and expand. The myocardium contains specialized conductive fibers which allow the rapid transmission of electrical pulses which cause the heart to contract.

- C. The epicardium is an exterior layer which covers the myocardial layer. There are also a few other layers surrounding the epicardium. The parietal epicardium is a membrane that acts like a protective sac and surrounds the heart. The most exterior layer is the fibrous pericardium which is also a sac that contains the heart.

Its functions are to provide another protective layer to the heart, to keep the heart contained in the chest cavity and to prevent the heart from over expanding. Inside the left ventricle we find the papillary muscles which control the closing and opening of the mitral valves. Moreover, we also find inside the ventricles trabeculae which are tissue projections of the ventricles' myocardium. Trabeculae can present themselves as surface elevations with grooves between them or as ridges on the ventricular wall which are floating inside the ventricle's cavity. The presence of papillary muscles and trabeculae in an image tend to make the automatic image analysis by computers much more difficult.

In this paper we are interested in segmenting the left ventricle's endocardium and epicardium from short axis MR images. In other words, we try to trace the membranes making up the endocardium and epicardium in a series of cardiac images. Often in clinical practice, the segmentation contours are drawn behind the papillary muscles and trabeculae [8]. Some authors choose to include the trabeculae and papillary muscles as part of the contour. Other authors have adopted the convention that we should consider the trabeculae and papillary muscles as part of the myocardium only when they are not freely "floating" in the ventricles' cavity [9]. Moreover, the epicardium is sometimes covered by a layer of fat, which makes the segmentation even more difficult. Depending on the cardiac function descriptor we are trying to estimate (see next section), this choice might have an effect on the final measures we get. In this thesis we adopt the convention followed in [8], and we assume that all the endocardial contours will be drawn behind the papillary muscles and trabeculae.

The heart contracts and expands periodically. A cardiac cycle is divided into two stages, the diastole and systole. Diastole represents the period when the ventricles are filling or a period when the ventricles are relaxing just prior to them being full. Systole represents the period when contraction occurs and the blood is ejected from the ventricle. These periods can be more finely analyzed, and we typically divide the cardiac cycle into seven phases.

These phases are:

1. Atrial
2. Contraction,
3. Isovolumetric contraction,
4. Rapid ejection,
5. Reduced ejection,
6. Isovolumetric relaxation,
7. Rapid filling and reduced filling.

The first system for automatically classifying these phases from a series of medical images was the ALVEN system [10]. Describing in detail these seven phases is beyond the scope of this paper. We wish to define, however, end-diastole and end-systole. By definition end-diastole occurs after the atrial contraction phase is complete, at which point the valves start to float upward, and the ventricular volumes are maximal. The volume of the LV at this point is called its end-diastolic volume (EDV). During the isovolumetric relaxation phase, the contraction of the ventricles is complete, and the pressure in the ventricles begins to decrease. At this phase, pressure changes cause the aortic valve and pulmonary valve to close. At the point when all the valves of the heart are closed, and we have reached end-systole, the ventricles have the smallest volume. This volume is referred to as the end-systolic volume (ESV). The difference between EDV and ESV is referred to as the stroke volume. The base of the heart is made mostly of the left atrium and a small portion of the right ventricle [11]. From the base, the heart extends downwards, in a slightly conical fashion and it ends at the apex of the heart. Figure 1.7 is a long axis view of the heart. The long axis of the LV is defined by the axis which passes through the apex and the geometric centre of the base [12]. A short axis view consists of a plane which is perpendicular to this long axis. Figure 1.2 presents a short axis cardiac MR slice. Our data set consists of short axis images of the heart. An accurate determination of the long axis of the LV is crucial as its incorrect estimation can lead to erroneous results. This estimation of the long axis can be done manually or automatically [12, 13].

2.4. Descriptors of Cardiac Function

In this section we will present the main descriptors of cardiac function. Cardiac models are typically used to obtain such cardiac performance descriptors and we will be reviewing some of these models in the next section.

Two of the main indicators of cardiac performance are the *Left Ventricular Volume (LVV)* and the *Left Ventricular Mass (LVM)*. As its name suggests LVV is the volume inside the left ventricle's chamber at a certain instant of the cardiac cycle. The best methods for estimating this have given relative errors ranging from 5.9% to 26.6% depending on the phase of the cardiac cycle where we are estimating the volume [14], the implementation, and the number of short axis slices used in the computation. LVM characterizes the mass of the left ventricle's myocardium. It can be determined by the total volume enclosed by the LV (the endocardial volume and the myocardium's volume), minus the LV's endocardial volume, all this multiplied by a constant to account for the density of the muscle mass, usually given as 1.05g/cm³ [14]. An abnormal value for LVM can be an indicator of cardiovascular disease.

The Ejection Fraction (EF) is considered one of the most meaningful measures of the LV's pump performance. It is defined as

$$EF = \frac{EDV - ESV}{EDV} \times 100\% \tag{1}$$

Where EDV is the end-diastolic volume enclosed by the endocardium, and ESV is the end-systolic volume enclosed by the endocardium. This can be applied either to the RV or the LV, with the LV's EF being more important, since as we mentioned above, most diseases typically arise in the LV. Typical values of EF are 67 ± 5% for the left ventricle and 61 ± 7% for the right ventricle, with abnormal values being an indication of cardiac disease. All these descriptors of cardiac function depend on an accurate segmentation of the cardiac ventricles, making the accurate segmentation of the LV's endocardium and epicardium extremely important. As already mentioned though, manual segmentation is a slow and error prone procedure, which is why automated methods for performing it are highly desirable.

2.4.1. Database

sunnybrook cardiac data (SCD) as also known as the 2009 cardiac MRI LV Segmentation challenge data . Consist of the 45 cine MRI Images from a Mixed of patients and Pathology Healthy, hypertrophy, heart failure, with infarction and heart failur without infraction. the data contributor is the image research, sunnybrook helth science center toranto, canada. the subset of the data where first used for automated mycoardium segmintation challenge form short axis MRI, held by a MICCAI workshop Now available on the CAP server with public doain licence. sunnybrook cardiac data (SCD) as also known as the 2009 cardiac MRI LV Segmentation challenge data . Consist of the 45 cine MRI Images from a Mixed of patients and Pathology Healthy, hypertrophy, heart failure, with infarction and heart failur without infraction. the data contributor is the image research, sunnybrook helth science center toranto, canada. the subset of the data where first used for automated mycoardium segmintation challenge form short axis MRI, held by a MICCAI workshop Now available on the CAP server with public doain licence.

Patient ID	Original ID	Gender	Age	Pathology
SCD0000101	SC-HF-I-1	Male	53	Heart failure with infarct
SCD0000201	SC-HF-I-2	Male	48	Heart failure with infarct
SCD0000301	SC-HF-I-4	Male	79	Heart failure with infarct
SCD0000401	SC-HF-I-5	Male	45	Heart failure with infarct
SCD0000501	SC-HF-I-6	Male	60	Heart failure with infarct
SCD0000601	SC-HF-I-7	Male	74	Heart failure with infarct
SCD0000701	SC-HF-I-8	Male	46	Heart failure with infarct
SCD0000801	SC-HF-I-9	Male	57	Heart failure with infarct
SCD0000901	SC-HF-I-10	Male	69	Heart failure with infarct
SCD0001001	SC-HF-I-11	Male	55	Heart failure with infarct
SCD0001101	SC-HF-I-12	Female	71	Heart failure with infarct
SCD0001201	SC-HF-I-40	Male	77	Heart failure with infarct
SCD0001301	SC-HF-NI-3	Female	81	Heart failure without infarct
SCD0001401	SC-HF-NI-4	Male	77	Heart failure without infarct
SCD0001501	SC-HF-NI-7	Male	81	Heart failure without infarct
SCD0001601	SC-HF-NI-11	Male	71	Heart failure without infarct
SCD0001701	SC-HF-NI-12	Female	63	Heart failure without infarct
SCD0001801	SC-HF-NI-13	Female	68	Heart failure without infarct
SCD0001901	SC-HF-NI-14	Male	82	Heart failure without infarct
SCD0002001	SC-HF-NI-15	Male	27	Heart failure without infarct
SCD0002101	SC-HF-NI-31	Male	52	Heart failure without infarct
SCD0002201	SC-HF-NI-33	Male	47	Heart failure without infarct
SCD0002301	SC-HF-NI-34	Male	52	Heart failure without infarct
SCD0002401	SC-HF-NI-36	Female	77	Heart failure without infarct

SCD0002501	SC-HYP-1	Male	83	Hypertrophy
SCD0002601	SC-HYP-3	Male	42	Hypertrophy
SCD0002701	SC-HYP-6	Female	46	Hypertrophy
SCD0002801	SC-HYP-7	Male	61	Hypertrophy
SCD0002901	SC-HYP-8	Male	62	Hypertrophy
SCD0003001	SC-HYP-9	Female	48	Hypertrophy
SCD0003101	SC-HYP-10	Male	47	Hypertrophy
SCD0003201	SC-HYP-11	Female	53	Hypertrophy
SCD0003301	SC-HYP-12	Female	76	Hypertrophy
SCD0003401	SC-HYP-37	Female	68	Hypertrophy
SCD0003501	SC-HYP-38	Male	38	Hypertrophy
SCD0003601	SC-HYP-40	Male	68	Hypertrophy
SCD0003701	SC-N-2	Male	63	Normal
SCD0003801	SC-N-3	Female	53	Normal
SCD0003901	SC-N-5	Female	77	Normal
SCD0004001	SC-N-6	Male	70	Normal
SCD0004101	SC-N-7	Male	23	Normal
SCD0004201	SC-N-9	Male	51	Normal
SCD0004301	SC-N-10	Male	61	Normal
SCD0004401	SC-N-11	Male	60	Normal
SCD0004501	SC-N-40	Female	88	Normal

Table 1 Subject information table [15].

	N (n=9)	HYP (n=12)	HF (n=12)	HF-I (n=12)
EDV (ml)	115.69 ± 36.89	114.39 ± 50.46	233.67 ± 63.21	244.92 ± 86.02
ESV (ml)	43.10 ± 14.74	43.11 ± 24.50	158.28 ± 56.34	174.34 ± 90.64
EF (%)	62.93 ± 3.65	62.72 ± 9.22	33.09 ± 13.07	32.01 ± 12.27

Table2. Classification of Min / Max.

2.5. Classification

The study description indicates the classification. The patient datasets were classified into four groups representing diverse morphologies, based on the following clinical criteria Heart failure with infarction (SC-HF-I) group had EF<40% and evidence of late gadolinium (Gd) enhancement Heart failure with no infarction(SC-HF-NI)group had EF < 40 % and no late Gd enhancement. LV hypertrophy (SC-HYP) group had normal LV ejection fraction (> 55%) and a ratio of LV mass / body surface area > 83 g/m² Healthy (SC- N) group had EF > 55% and no hypertrophy.

2.6. Result: Experiment Work Cardiac LV Segmentation using SIOX

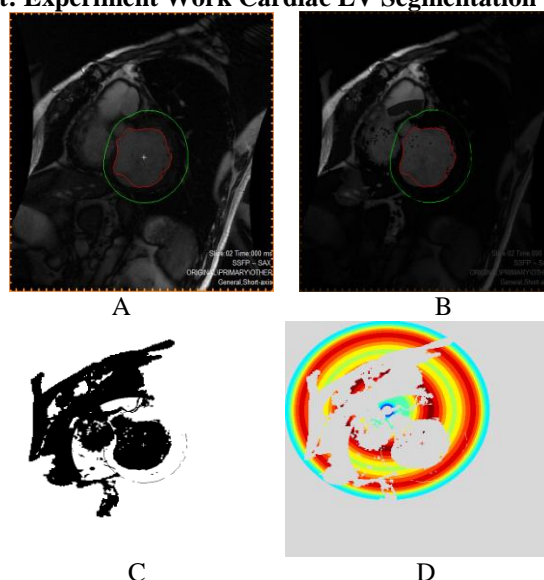


Figure1.8 Automatic Segmentation techniques result using SIOX techniques. (A) SIOX-Seed point Segmented image (B) show Foreground / Background (C) Thresholding (D) result in shall analysis MASK

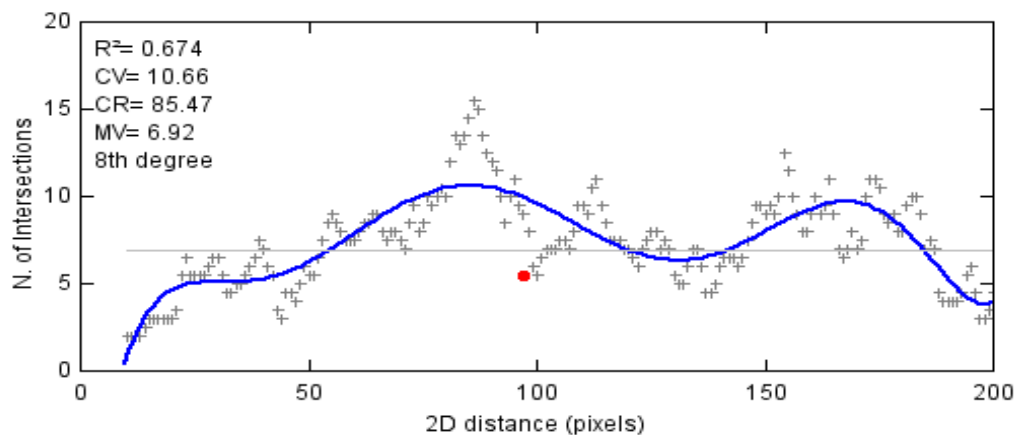


Figure1.9 Graphical Result Log-Log Analysis

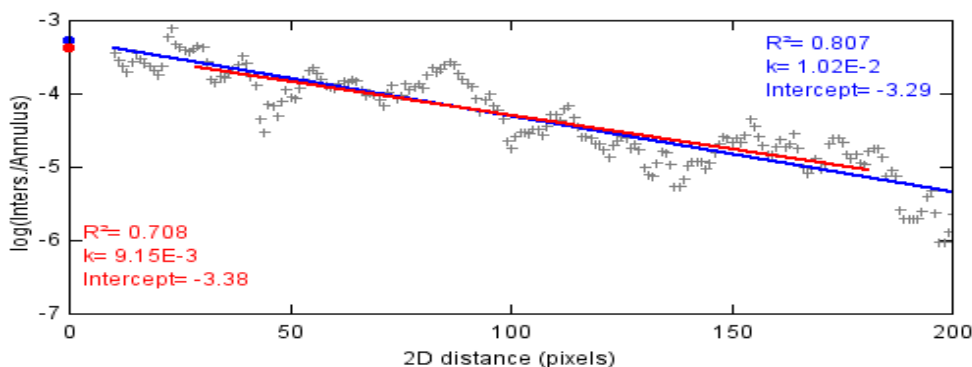


Figure1.10 Graphical Result Linear Analysis

Result: Endocardium / Epicardium using semi-Automatic Segmentation Techniques give the 100% result accuracy compare the Sunnybrook result following SIOX using result.

Endocardium

Mean	4.84E+03	8.38E+01	1.51E+01	8.26E+01
SD	2.33E+03	2.51E+01	6.77E+00	2.26E+01
Min	9.12E+02	4.26E+01	6.97E+00	3.50E+01
Max	1.23E+04	1.64E+02	3.77E+01	1.65E+02

Epicardium

Mean	9.67E+03	6.07E+01	2.91E+01	7.74E+01
SD	3.94E+03	2.01E+01	7.66E+00	2.12E+01
Min	3.80E+03	2.81E+01	1.63E+01	7.00E+00
Max	2.32E+04	1.30E+02	4.92E+01	8.50E+01

Table 3 Result table using SIOX algorithm

III. Conclusions

We are using SIOX ROI Techniques for got good result as compare to other techniques; the proposed technique automatically and rapidly detects endocardial, epicardial, papillary muscles' and trabeculations' contours providing accurate and reproducible quantitative MRI parameters, including LV mass and EF.

IV. Future work

Today our environment increasing pollution, loos the fruit quality, day by day increase cardiac problem, this problem how overcome using Left and Right MRI for fusion concept.

Key Words: Left ventricular ejection fraction (LVEF), left ventricular mass (LVM), cardiac magnetic resonance imaging (CMRI), automated border detection (ABD), image processing(IP).

References

- [1] Jeffrey L. Anderson, Aaron N. Weaver, Benjamin D. Horne, Heath U. Jones, Gerri K. Jelaco, Julie A. Cha, Hector E. Busto, Judy Hall, Kathy Walker, and Duane D. Blatter. Normal cardiac magnetic resonance measurements and interobserver discrepancies in volumes and mass using the papillary muscle inclusion method. *The Open General and Internal Medicine Journal*, 1:6–12, 2007.
- [2] M.D. Burkhard Sievers, Simon Kirchberg, Asli Bakan, M.D. Ulrich Franken, and M.D. Hans-Joachim Trappe. Impact of papillary muscles in ventricular volume and ejection fraction assessment by cardiovascular magnetic resonance. *Journal of Cardiovascular Magnetic Resonance*, 6(1):9–16, 2004.
- [3] Matthew Janik, Matthew D Cham, Michael I Ross, Yi Wang, Noel Codella, James K Min, Martin R Prince, Shant Manoushagian, Peter M Okin, Richard B Devereux, and Jonathan W Weinsaft. Effects of papillary muscles and trabeculae on left ventricular quantification: increased impact of methodological variability in patients with left ventricular hypertrophy. *Journal of Hypertension*, 26(8):1677–1685, August 2008.
- [4] Mendis S., Puska P., and Norrving B., editors. *Global Atlas on Cardiovascular Disease Prevention and Control*. World Health Organization, Geneva, 2011.
- [5] Prediman K. Shah, Jamshid Maddahi, Howard M. Staniloff, A. Gray Ellrodt, Max Pichler, H.J.C. Swan, and Daniel S. Berman. Variable spectrum and prognostic implications of left and right ventricular ejection fractions in patients with and without clinical heart failure after acute myocardial infarction. *The American Journal of Cardiology*, 58(6):387–393, 1986.
- [6] J Vogel-Claussen, JP Finn, AS Gomes, GW Hundley, M Jerosch-Herold, G Pearson, S Sinha, JA Lima, and DA Bluemke. Left ventricular papillary muscle mass: relationship to left ventricular mass and volumes by magnetic resonance imaging. *Journal of Computer Assisted Tomography*, 30(3), May 2006.
- [7] Ionizing radiation. World health organization. [Online]: <http://www.who.int/ionizing radiation/en/>.
- [8] S. C. Mitchell, J. G. Bosch, B. P. F. Lelieveldt, R. J. van der Geest, J. H. C. Reiber, and M. Sonka. 3-D Active Appearance Models: Segmentation of Cardiac MR and Ultrasound Images. *IEEE Transactions on Medical Imaging*, 21(9):1167–1178, 2002.
- [9] Marie-Pierre Jolly, Nicolae Duta, and Gareth Funka-Lee. Segmentation of the Left Ventricle in Cardiac MR Images. In *International Conference on Computer Vision*, 2001.
- [10] J. K. Tsotsos. *A Framework for Visual Motion Understanding*. PhD thesis, University of Toronto, Department of Computer Science, 1980.
- [11] C. Rosse and P. Gaddum-Rosse. *Hollinshead's textbook of anatomy*. Lippincott-Raven, 5th edition, 1997.
- [12] R. A. deKemp and C. Nahmias. Automated determination of the left ventricular long axis in cardiac positron tomography. *Physiol. Meas.*, 17:95–108, 1996.
- [13] B.P.F Lelieveldt et al. Automated observer-independent acquisition of cardiac short axis mr images. *Radiology*, pages 537–542, 2001.
- [14] A. F. Frangi, W.J. Niessen, and M. A. Viergever. Three dimensional modeling for functional analysis of cardiac images: A review. *IEEE Transactions on Medical Imaging*, 20(1):2–25, 2001.
- [15] Kayte jaypalsing et al. “Left Ventricle Statistical Models Segmentation of Shape and Appearance for Analysis of Cardiac MRI” *International Journal of Computer Applications* (0975 – 8887) Volume 104 – No.7, October 2014
- [16] url database <http://sunnybrook.ca/>